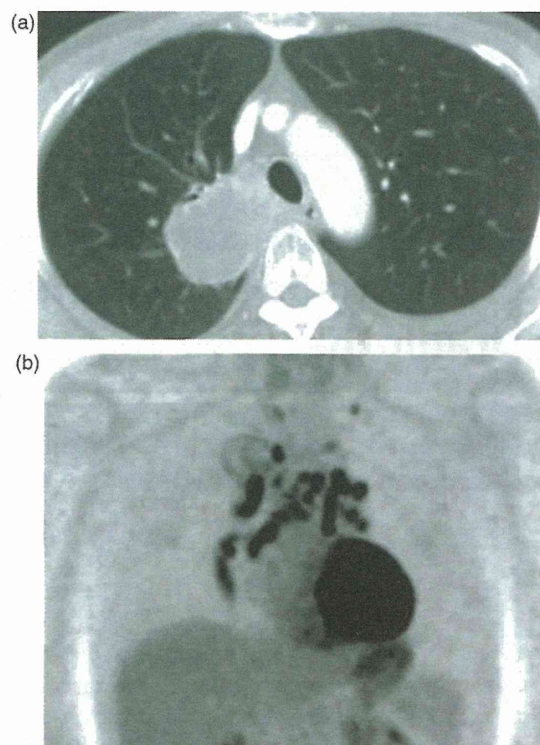


**Figure 1.** (a) Computed tomography scan showing a mass lesion measuring 55 mm in diameter in the right upper lobe and a single hilar lymphadenopathy. (b) Positron-emission tomography showing  $^{18}\text{F}$ -fluorodeoxyglucose accumulation in the lung tumor and one hilar lymph node.



**Figure 2.** (a) Computed tomography scan showing that the primary tumor had reduced in size to 44 mm, and the hilar lymph node had not changed in size. (b) Positron-emission tomography showing little  $^{18}\text{F}$ -fluorodeoxyglucose accumulation in the lung tumor, but high accumulation in the mediastinal lymph nodes.

changed in size (Figure 2(a)). On the other hand, FDG-PET demonstrated little accumulation in the lung tumor but high accumulation in many mediastinal lymph nodes (Figure 2(b)). To differentiate from disease progress, we performed a biopsy of the mediastinal lymph nodes by mediastinoscopy. Histologically, all sampled lymph nodes showed epithelioid granuloma consisting of histiocytes, lymphocytes, and fibroblasts. With the decision that induction therapy had been effective, we performed a right upper lobectomy and systemic mediastinal lymph node dissection. Pathological findings of the tumor showed necrosis and epithelioid granuloma consisting of fibroblasts, histiocytes, and lymphocytes. No viable tumor cells were identified (Figure 3(a)). Pathological findings of the dissected lymph nodes showed necrosis and proliferation of fibroblasts, histiocytes, and multinuclear giant cells (Figure 3(b)). The patient was finally diagnosed with a complete pathological response to induction therapy, and sarcoid reaction following induction therapy was suggested in the mediastinal lymph nodes. He had no serious complication in the postoperative course. Six weeks later, he received 2 cycles of adjuvant chemotherapy consisting of cisplatin plus irinotecan.

## Discussion

A localized epithelioid granuloma without signs of systemic sarcoidosis has been called "sarcoid reaction," although such lesions are rarely observed in the regional draining lymph nodes of a malignant tumor. The overall incidence of this reaction in patients with carcinoma has been reported to be 4.4%.<sup>2</sup> With regard to lung cancer patients, Laurberg<sup>3</sup> reported that 20 of 630 (3.2%) patients had sarcoid reactions in mediastinal lymph nodes. Some studies have shown that sarcoid reactions are also observed within the primary tumor in patients with lung cancer.<sup>4,5</sup> Aoki and colleagues<sup>4</sup> mentioned that the histologic type of all reported cases was adenocarcinoma. On the other hand, it has been reported that the majority of patients with sarcoid reactions in regional lymph nodes had squamous cell carcinoma.<sup>5</sup> A possible explanation could be that squamous cell carcinoma grows more slowly than other types of carcinoma, and regional lymph nodes are exposed to the lymph flow from lung cancer for a longer period.<sup>5</sup> The pathogenesis of sarcoid reactions remains unclear. Brincker<sup>2</sup> reported that tumor-associated sarcoid reactions do not contribute to a direct interaction between tumor cells and lymph nodes, because this reaction commonly occurred in



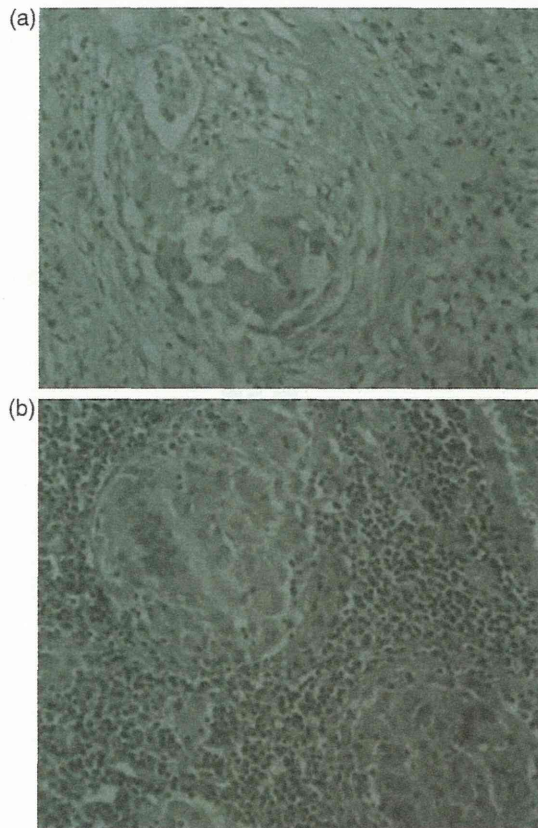


**Figure 3.** (a) Pathological findings of the tumor showed necrosis and epithelioid granuloma consisting of fibroblasts, histiocytes, and lymphocytes, and no viable tumor cells. Hematoxylin and eosin stain, original magnification  $\times 100$ . (b) Pathological findings of dissected lymph nodes showing necrosis and epithelioid granuloma consisting of fibroblasts, histiocytes, and lymphocytes, and multinuclear giant cells. Hematoxylin and eosin stain, original magnification  $\times 100$ .

lymph nodes without metastasis. Therefore, sarcoid reactions may be caused by soluble antigenic factors derived from tumor cells.

FDG-PET has been shown to be useful for diagnosis of lymph node metastasis and evaluation of induction chemoradiotherapy for lung cancer. Silvestri and colleagues<sup>6</sup> reported that the pooled estimates of sensitivity and specificity of FDG-PET for identifying mediastinal metastasis were 74% and 85%, respectively. However, it has also been reported that FDG-PET provides false-positive results in cases of tuberculosis and sarcoidosis, as well as other inflammatory diseases.<sup>7</sup> In the present case, the accumulation of FDG in mediastinal and hilar

lymph nodes led us to suspect the progression of lung cancer after induction therapy. Maeda and colleagues<sup>8</sup> also reported that a sarcoid reaction in mediastinal lymph nodes led to false-positive accumulation of FDG without tumor metastasis. However, there has been no report of sarcoid reaction in the mediastinal lymph nodes following induction chemoradiotherapy. Treatment-related sarcoid reaction should be considered when the accumulation of FDG shows rapid expansion in the course of treatment. It should be noted that sarcoid reaction involving mediastinal lymph nodes can occur during chemoradiotherapy for lung cancer.

### Funding

This research received no specific grant from any funding agency in the public, commercial, or not-for-profit sectors.

### Conflicts of interest statement

None declared.

### References

1. Goo JM, Im JG, Do KH, et al. Pulmonary tuberculosis evaluated by means of FDG-PET: findings in 10 cases. *Radiology* 2000; 216: 117–121.
2. Brincker H. Sarcoid reaction in malignant tumors [Review]. *Cancer Treat Rev* 1986; 13: 147–156.
3. Laurberg P. Sarcoid reactions in pulmonary neoplasms. *Scand J Respir Dis* 1975; 56: 20–27.
4. Aoki K, Yoshimura K, Hoashi S, et al. Lung cancer with a sarcoid-like reaction in the primary lung cancer. *Nippon kyobu Shikkan Gakkai Zasshi* 1997; 35: 466–470.
5. Segawa Y, Takigawa N, Okahara M, et al. Primary lung cancer associated with diffuse granulomatous lesions in the pulmonary parenchyma. *Internal Med* 1996; 35: 727–731.
6. Silvestri GA, Gould MK, Margolis ML, et al. Noninvasive staging of non-small cell lung cancer: ACCP evidenced-based clinical practice guidelines (2nd edition). *Chest* 2007; 132(Suppl 3): 178S–201S.
7. Hellwig D, Graeter TP, Ukena D, Georg T, Kirsch CM and Schafers HJ. Value of <sup>18</sup>F fluorodeoxyglucose positron emission tomography after induction therapy of locally advanced bronchogenic carcinoma. *J Thorac Cardiovasc Surg* 2004; 128: 892–899.
8. Maeda J, Ohta M, Hirabayashi H and Matsuda H. False positive accumulation in <sup>18</sup>F fluorodeoxyglucose positron emission tomography scan due to sarcoid reaction following induction chemotherapy for lung cancer. *Jpn J Thorac Cardiovasc Surg* 2005; 53: 196–198.

# Clinical significance of the tumor microenvironment in non-small cell lung cancer

Katsuhiko Shimizu, Riki Okita, Masao Nakata

Department of General Thoracic Surgery, Kawasaki Medical School, Kurashiki, Japan

Corresponding to: Katsuhiko Shimizu. Department of General Thoracic Surgery, Kawasaki Medical School, 577 Matsushima, Kurashiki Okayama 701-0192, Japan. Email: kshimizu@med.kawasaki-m.ac.jp.

**Abstract:** Several biomarkers have been reported as predictors of survival and recurrence in non-small cell lung cancer. Recently, several groups have demonstrated that the immune microenvironment of the primary tumors is a prognostic factor. These “immunological biomarkers” in the tumor microenvironment are useful predictors of prognosis as well as promising targets for novel therapeutic approaches. Especially, tumor-infiltrating Treg cells are a powerful immunological biomarker, and possible mechanisms involved in the induction of tumor-infiltrating Treg cells are the expression of Cox-2, IL-12R $\beta$ 2 or the lack of IL7R on the tumor cells. These findings may pave the way for individualized immunomodulatory therapies to deplete tumor-infiltrating Treg cells from the tumor microenvironment.

**Key Words:** Non-small cell lung cancer (NSCLC); tumor microenvironment; tumor-infiltrating Treg



Submitted May 15, 2013. Accepted for publication Jun 04, 2013.

doi: 10.3978/j.issn.2305-5839.2013.06.01

Scan to your mobile device or view this article at: <http://www.atmjournals.org/article/view/2192/3011>

This editorial refers to the ‘Clinical Impact of Immune Microenvironment in Stage I Lung Adenocarcinoma: Tumor Interleukin-12 Receptor 2 (IL-12R2), IL-7R, and Stromal FoxP3/CD3 Ratio Are Independent Predictors of Recurrence’ by K. Suzuki *et al.*, published in the *Journal of Clinical Oncology* (1).

Lung cancer is a major cause of death in many developed countries. Surgical resection continues to play an important role in the treatment of this disease, especially during the early stages of non-small cell lung cancer (NSCLC). Even in patients diagnosed at an early stage, however, the reported relapse rate is as high as 15-35% after surgical resection. Therefore, the prognostic factors of NSCLC patients following resection have been investigated. Until now, the anatomic extent of the tumor (TNM classification) has been the most powerful tool to predict the prognosis in NSCLC patients. Several biomarkers have been reported as predictors of survival and recurrence: (I) clinical factors (e.g., sex, age, or performance-status); (II) pathological factors (e.g., histological subtype, cell differentiation, or visceral pleural invasion); (III) many biological factors involved in

cancer development and progression (e.g., *EGFR* mutation). Recently, several groups, including ours, have demonstrated that the immune microenvironment of the primary tumors is a prognostic factor for disease-free and overall survival. Thus, the tumor immune microenvironment has been increasingly considered as a biomarker of the prognosis, as well as a therapeutic target in patients with NSCLC.

## Tumor-infiltrating immune cells

It is composed of two distinct compartments mediating the innate and adaptive immune responses. The innate immune system consists of phagocytes including neutrophils, mast cells/macrophages (CD68), dendritic cells (DC), NK cells (CD56+CD3-), and NK T cells (CD56+CD3+). The innate immune system mainly serves as the first-line defense against both foreign pathogens and transformed cells. The adaptive immune system is mediated by two major T lymphocyte subsets; cytotoxic T cells (CTL) (CD8) and helper T cells (Th) (CD4), and B cells (CD20). The adaptive immune system is the second-line of defense via



antigen-specific molecules which requires clonal expansion following the recognition of foreign antigens.

Of these, tumor-infiltrating DCs (2,3), NK cells (3), macrophages (4), mast cells (5), cytotoxic T cells (6), and helper T cells (7) have been reported as potential prognostic factors following resection in patients with NSCLC. In addition, we recently reported that the number of tumor infiltrating FOXP3<sup>+</sup> Treg cells was associated with earlier recurrence, especially in patients with node-negative NSCLC, and positively correlated with Cox-2 expression on the tumor cells (8). Therefore, we suggested that Cox-2 expressed in tumors is a possible target for decreasing the number of tumor-infiltrating Treg cells.

### Tumors expressing cytokine receptors

The interactions between cancer cells and the tumor microenvironment are bidirectional, and include activation of both tumor and accessory stromal cells. These interactions are crucial for cancer progression. In order to create a suitable tumor microenvironment, cancer cells communicate with the microenvironment via a complex network of many growth factors, chemokines, cytokines, and their own receptors.

Chemokines and chemokine receptors play important roles in tumor progression. Both cancer cells and stromal cells elaborate several chemokines and cytokines. Expressions of CXCR4 and its ligand CXCL12 have been reported in some solid tumors. Clinical data indicate that high CXCR4 expression is correlated with poor clinical outcome in several cancers. The proposed paracrine roles for the CXCR4/CXCL12 axis are to assist in facilitation of the development of distant metastasis, while the CCL21/CCR7 axis favors the development of lymph node metastasis. These two chemokine ligand-receptor interactions are reported as common key mediators of tumor cell metastasis in several types of cancers. Thus, both CXCR4 and CCR7 have been implicated in the process of metastasis; however, the potential prognostic values of these molecules in resected NSCLC are unknown. Previous studies have assessed the relationship between the concentrations of cytokines in the serum and the clinicopathological factors in NSCLC patients; however, there are few studies that have assessed the expressions of cytokine receptors on the tumor cells. The interleukin-7 receptor (IL-7R) provides critical survival signals to lymphocytes, while IL-12R $\beta$ 2 acts not only as a cytokine receptor component, but also as a gatekeeper gene, since

lung adenocarcinoma develops spontaneously in IL-12R $\beta$ 2 deficient mice.

Of these, IL-7R expression on the tumor cells has been reported to be associated with a shorter overall survival in NSCLC patients (9), while *IL-12R $\beta$ 2* methylation has been shown to be correlated with a poor prognosis in lung adenocarcinoma patients (10).

A previous study showed that the type, density, and location of immune cells within the tumor microenvironment influence the risk of recurrence. Suzuki *et al.* additionally demonstrated that the expressions of the cytokine receptor IL-7R and IL-12R $\beta$ 2 on the tumor cells are also useful predictive prognostic factors following resection in patients with NSCLC. Taken together, “Immunological biomarkers” in the tumor microenvironment are useful predictors of prognosis as well as promising targets for novel therapeutic approaches. Tumor-infiltrating FOXP3<sup>+</sup> Treg cells are a powerful immunological biomarker for the predicting prognosis following resection in patients with NSCLC. Recent studies have suggested possible mechanisms involved in the induction of tumor-infiltrating Treg cells are the expression of Cox-2, IL-12R $\beta$ 2 or the lack of IL7R on the tumor cells. These findings may pave the way for individualized immunomodulatory therapies using the Cox-2 inhibitor, IL-12R $\beta$ 2 stimulator, or the IL-7R inhibitor to deplete tumor-infiltrating Treg cells from the tumor microenvironment.

### Acknowledgements

*Disclosure:* The authors declare no conflict of interest.

### References

1. Suzuki K, Kadota K, Sima CS, et al. Clinical impact of immune microenvironment in stage I lung adenocarcinoma: tumor interleukin-12 receptor  $\beta$ 2 (IL-12R $\beta$ 2), IL-7R, and stromal FoxP3/CD3 ratio are independent predictors of recurrence. *J Clin Oncol* 2013;31:490-8.
2. Dieu-Nosjean MC, Antoine M, Danel C, et al. Long-term survival for patients with non-small-cell lung cancer with intratumoral lymphoid structures. *J Clin Oncol* 2008;26:4410-7.
3. Al-Shibli K, Al-Saad S, Donnem T, et al. The prognostic value of intraepithelial and stromal innate immune system cells in non-small cell lung carcinoma. *Histopathology* 2009;55:301-12.

4. Dai F, Liu L, Che G, et al. The number and microlocalization of tumor-associated immune cells are associated with patient's survival time in non-small cell lung cancer. *BMC Cancer* 2010;10:220.
5. Takanami I, Takeuchi K, Naruke M. Mast cell density is associated with angiogenesis and poor prognosis in pulmonary adenocarcinoma. *Cancer* 2000;88:2686-92.
6. Al-Shibli KI, Donnem T, Al-Saad S, et al. Prognostic effect of epithelial and stromal lymphocyte infiltration in non-small cell lung cancer. *Clin Cancer Res* 2008;14:5220-7.
7. Wakabayashi O, Yamazaki K, Oizumi S, et al. CD4+ T cells in cancer stroma, not CD8+ T cells in cancer cell nests, are associated with favorable prognosis in human non-small cell lung cancers. *Cancer Sci* 2003;94:1003-9.
8. Shimizu K, Nakata M, Hiramami Y, et al. Tumor-infiltrating Foxp3+ regulatory T cells are correlated with cyclooxygenase-2 expression and are associated with recurrence in resected non-small cell lung cancer. *J Thorac Oncol* 2010;5:585-90.
9. Ming J, Zhang Q, Qiu X, et al. Interleukin 7/interleukin 7 receptor induce c-Fos/c-Jun-dependent vascular endothelial growth factor-D up-regulation: a mechanism of lymphangiogenesis in lung cancer. *Eur J Cancer* 2009;45:866-73.
10. Suzuki M, Iizasa T, Nakajima T, et al. Aberrant methylation of IL-12Rbeta2 gene in lung adenocarcinoma cells is associated with unfavorable prognosis. *Ann Surg Oncol* 2007;14:2636-42.

**Cite this article as:** Shimizu K, Okita R, Nakata M. Clinical significance of the tumor microenvironment in non-small cell lung cancer. *Ann Transl Med* 2013;1(2):20. doi: 10.3978/j.issn.2305-5839.2013.06.01



## Role of 2-[18F]fluoro-2-deoxyglucose positron emission tomography in preoperative management of solid-type small-sized lung cancer

Shinsuke Saisho · Koichiro Yasuda ·  
Ai Maeda · Takuro Yukawa · Riki Okita ·  
Yuji Hiramami · Katsuhiko Shimizu · Masao Nakata

Received: 10 January 2013 / Accepted: 27 February 2013 / Published online: 16 March 2013  
© The Japanese Society of Nuclear Medicine 2013

### Abstract

**Objective** 2-[18F]Fluoro-2-deoxyglucose positron emission tomography (FDG-PET) is routinely used for the diagnosis of primary lung cancer. However, the role of FDG-PET in the diagnosis and staging of small-sized lung cancer has not been sufficiently evaluated. The purpose of this study was to determine the utility of FDG-PET for preoperative staging of solid-type small-sized lung cancer manifesting as solid-component predominant nodules.

**Methods** One-hundred and eighteen patients with solid-type small-sized ( $\leq 2$  cm) lung cancer diagnosed as clinical stage IA based on thin-slice computed tomography (TS-CT) were included in this study. Before surgery, FDG-PET was performed in 78 patients (CT/PET group), and TS-CT alone was performed in 40 patients (CT group). Clinical and pathological stage and prognosis were retrospectively reviewed according to whether FDG-PET had been performed.

**Results** No significant differences in clinical factors were observed when comparing the CT/PET group and the CT group. Of the 78 patients in the CT/PET group, 12 (15.4 %) were diagnosed with clinical stage IIA or IIIA disease based on FDG-PET findings, but no advanced cases with contraindications for curative surgery were seen. In the CT/PET group, the pathological stage was IA in 66 patients, IB in eight patients, IIA in one patient, and IIIA in three patients; 16 patients had incorrectly staged disease. The accurate staging rate was 79.5 % for the CT-PET group

and 70.0 % for the CT group ( $P = 0.262$ ). Among patients diagnosed with clinical stage IA disease, the 3-year overall survival rate was 85.5 % for the 66 patients in the CT/PET group and 76.8 % for the 40 patients in the CT group ( $P = 0.554$ ). No significant difference was observed in accuracy of preoperative staging and prognosis between the two groups.

**Conclusions** FDG-PET produced no clear benefit for the preoperative management of patients with solid-type clinical T1aN0M0 lung cancer, in terms of postoperative survival and the concordance rate of clinical and pathological stage.

**Keywords** Small-sized lung cancer · Preoperative staging · FDG-PET · CT

### Introduction

2-[18F]Fluoro-2-deoxyglucose positron emission tomography (FDG-PET) is a noninvasive diagnostic technique with the potential to improve preoperative staging of primary lung cancer. Since its introduction in the 1990s, FDG-PET has been rapidly adopted for and widely used in standard diagnostic work-ups for primary lung cancer. Currently, this modality plays an important role in differentiating malignant and benign pulmonary nodular lesions and diagnosing lymph node metastases, distant metastases, and postoperative recurrences [1–4]. The major feature of FDG-PET is its ability to be used for whole-body evaluations. Thus, FDG-PET has been well established as a noninvasive modality for diagnosing recurrence as well as for the assessment of the primary tumor, lymph node involvement, and distant metastasis in patients with primary lung cancer.

S. Saisho (✉) · K. Yasuda · A. Maeda · T. Yukawa · R. Okita ·  
Y. Hiramami · K. Shimizu · M. Nakata  
Department of General Thoracic Surgery, Kawasaki Medical  
School Hospital, 577 Matsushima, Kurashiki,  
Okayama 701-0192, Japan  
e-mail: s.saisho@med.kawasaki-m.ac.jp

Recent studies have shown that FDG-PET can provide high specificity and positive predictive value in lymph node staging even in patients with cT1 lung cancer [5, 6]. However, these previous studies of FDG-PET for lymph node staging have been performed without considering the size or characteristics of the primary tumors. In this context, the diagnostic value of FDG-PET for solid-component predominant small-sized lung cancers measuring 2 cm or less (cT1a) may be different from that for larger lung cancers. This is an increasingly relevant issue, as the proportion of all lung cancers comprising small-sized lung cancers has increased [7]. There have been only a few studies dealing with this topic, and none of them have compared the use of FDG-PET and computed tomography (CT) for preoperative evaluation of small-sized cancers preoperatively. Further, the significance of FDG-PET for preoperative staging and prognosis of small-sized lung cancer has not been sufficiently studied [5, 6, 8–10].

Therefore, the purpose of this study was to retrospectively evaluate the diagnostic accuracy of FDG-PET for preoperative staging in solid-component predominant, small-sized lung cancers diagnosed as cT1aN0, stage IA based on thin-section CT (TS-CT) examination, and to compare the accuracies of FDG-PET and TS-CT in the preoperative staging of cT1N0 lung cancers. We also investigated whether or not there was a difference in outcomes of cT1aN0 lung cancer according to whether or not FDG-PET was used.

## Materials and methods

### Study population

Of 494 patients who underwent surgical resection at the Kawasaki Medical School Hospital, Kurashiki, Japan between January 2004 and December 2011, 118 consecutive patients with solid-type small-sized primary lung cancer who had been diagnosed with clinical T1aN0M0 (cT1aN0M0), stage IA disease based on a preoperative thoraco-abdominal CT were included in this study. “Solid-type” lung cancer was defined as a lesion with a solid component of more than 50 % on TS-CT. Patients with ground glass opacity (GGO) predominant (solid component 50 % or less) lesions were excluded.

The 118 patients were categorized into one of two groups: the CT group or the CT/PET group. The CT group consisted of 40 patients, who had surgery earlier than December 2006, had been staged preoperatively using contrast-enhanced CT, magnetic resonance imaging (MRI) of the brain, and bone scintigraphy. The CT/PET group consisted of 78 patients, who had surgery after January 2007 and who had been evaluated by CT, FDG-PET, and MRI of the brain. Routine mediastinoscopy or

endobronchial ultrasound with transbronchial needle aspiration to detect occult mediastinal lymph node metastases was not performed.

The clinical and pathological stage and postoperative survival were retrospectively evaluated between the two patient groups. The impact of FDG-PET on the therapeutic decision and surgical outcomes was also investigated. Clinical information was obtained from the patients’ medical records. Histology was categorized according to the World Health Organization Classification of Tumors, 3rd edition, and the TNM classification was assigned according to the International Union against Cancer staging system [11, 12].

Written informed consent was obtained from each patient, and the study protocol was approved by the Research Ethics Committee of Kawasaki Medical School and Hospital.

### Computed tomography

Chest CT was performed with two different scanners: 16-detector-row (LightSpeed 16; GE Healthcare, Milwaukee, Wis) or single-detector-row (Proseed SA Libra; GE Healthcare). Parameters for the 16-detector-row scanner were as follows: exposure setting, 323–432 mA, 0.5 s/rotation at 120 kVp; collimation,  $16 \times 0.625$  or 1.25 mm; and beam pitch, 1.75:1. Parameters for the single-detector-row scanner were as follows: exposure setting, 130–160 mA, 0.8 s/rotation at 140 kVp; collimation, 5 or 1 mm; beam pitch, 1.5:1. Thin-section (0.625–2.0 mm) images were reconstructed with no overlap using the bone convolution kernel and were transferred to our research picture archiving and communication system server.

For each hilar and mediastinal lymph nodes, the short-axis diameter of the nodes was measured using CT. Enlarged nodes, that were a short-axis diameter of 10 mm or larger on CT scan, were defined to metastasis.

### FDG-PET: imaging protocol and analysis

All PET/computed tomography examinations were performed with a dedicated PET/CT scanner (Discovery ST Elite; GE Healthcare, Kyoto, Japan). The axes of the multidetector CT and PET systems were mechanically aligned so that the patient could be moved from the CT to the PET scanner gantry by simply changing the position of the examination table. The resultant PET and CT scans were coregistered with hardware. PET/CT scanning was performed at 115 min after the intravenous injection of 150–220 MBq of 18-fluorodeoxyglucose (FDGscan, Nihon Medi-Physics, Tokyo, Japan). The regions of interest were placed 3-dimensionally over the lung cancer nodules. Semiquantitative analysis of the images was performed by



measuring the maximal standardized uptake values (SUVmax) of the primary tumor and lymph nodes. SUV was calculated on the basis of the following equation: tumor activity concentration/(injected dose/body weight).

Results of FDG-PET scans were considered “positive” in the mediastinum and hilar area that was separate from the primary mass if the SUVmax in patients suspected to have lymph node metastases was greater than 2.5 and exhibiting a left–right asymmetry [13].

Measurements of short-axis diameter on CT were performed by chest radiologists and calculations of FDG uptake on FDG-PET were performed by nuclear oncologists. These image interpretations were finally determined by board-certified thoracic surgeons.

#### Surgical procedures and adjuvant chemotherapy

Lobectomy with systematic or lobe-specific lymph node dissection (SND) was conducted in most patients. However, in high-risk patients, sublobar resection was selected. Adjuvant chemotherapy was indicated in patients with pII and pIIIA non-small cell lung cancer (NSCLC) or in patients with small cell lung cancer (SCLC) patients and good performance status.

#### Postoperative follow-up

A postoperative follow-up examination was performed every 3 months for the first 2 years, and every 6–12 months thereafter. Follow-up evaluations included a physical examination, determination of serum levels of carcinoembryonic antigen, and chest radiography. Screening examinations by CT or FDG-PET were performed every 6 or 12 months for at least 5 years. A diagnosis of recurrent disease was diagnosed based on a physical examination and diagnostic imaging such as CT, MRI, and/or FDG-PET.

#### Statistical analysis

The clinicopathological parameters of the CT/PET group and CT group were compared using a Chi-square test. Univariate analyses were performed using the log-rank test. The survival curves were drawn using the Kaplan–Meier method. Differences were considered significant at  $P \leq 0.05$ . SPSS was used for statistical analysis.

## Results

#### Clinical characteristics

The patients’ clinical characteristics are summarized in Table 1. No significant differences in patients’ clinical

**Table 1** Clinical characteristics of patients with clinical T1aN0M0 primary lung cancer

	CT/PET group N = 78	CT group N = 40	P value
Age (years)			0.797
Median	72.0	73.0	
Range	46–90	45–87	
Sex (%)			0.554
Male	52 (67)	24 (60)	
Female	26 (33)	16 (40)	
Smoking status (%)			0.674
Never-smoker	26 (33)	14 (35)	
Ex-/current-smoker	51 (65)	22 (55)	
Unknown	1 (1.3)	4 (10)	
Smoking index (pack-years)			
Median	42.0	58.1	
Range	0.3–125	19–125	
Tumor marker status			
CEA (ng/ml)			0.193
>5.0/≤5.0	21/55	15/21	
CYFRA (ng/ml)			0.126
>2.0/≤2.0	6/31	5/8	
proGRP (pg/ml)			>0.999
>46.0/≤46.0	6/21	3/12	

CEA carcinoembryonic antigen, CYFRA cytokeratin 19 fragment, proGRP pro-gastrin-releasing peptide

parameters, including age, sex, smoking status, and smoking index, were seen when comparing the two groups.

#### Preoperative radiologic findings

CT and FDG-PET findings and the final clinical stage are summarized in Table 2. In the CT/PET group, the maximum tumor dimension ranged from 9 to 20 mm (median, 16.0 mm), and 63 of 78 patients (80.8 %) had tumors that were purely solid on TS-CT. In the CT group, the maximum tumor dimension ranged from 8 to 20 mm (median, 17.0 mm), and 30 of 40 patients (75.0 %) had purely solid tumors. No significant differences in preoperative CT findings were seen when comparing the two groups.

The proportion of patients with FDG uptake in the primary lesion was 89.7 % (70 of 78 patients), and the value of the SUVmax ranged from 1.4 to 19.0 (median, 4.9). There were 12 patients with PET-positive hilar/mediastinal lymph nodes. Based on CT and FDG-PET results, the final clinical stage was IA (cT1aN0M0) disease in 66 patients, cIIA (cT1aN1M0) in six patients, and cIIIA (cT1aN2M0) in six patients. In 12 of 78 patients (15.4 %) in the CT/PET group, the final clinical stage was up-staged from conventional CT staging, but none of the cases were diagnosed



**Table 2** Radiographic findings and clinical stage

	CT/PET group N = 78	CT group N = 40	P value
Size on CT (mm)			0.965
Median	16.0	17.0	
Range	9–20	8–20	
HRCT findings (%)			0.483
Pure solid lesion	63 (81)	30 (75)	
Solid component-dominant lesion	15 (19)	10 (25)	
FDG-PET findings			
Primary tumor			
FDG uptake (+), (%)	70 (90)		
SUVmax			
Median	4.9		
Range	1.4–19.0		
Hilar/Mediastinal lymph node			
FDG uptake (+), (%)	12 (15)		
SUVmax			
Median	4.1		
Range	2.8–8.8		
Clinical stage (%)			
cT1aN0M0, stage IA	66 (84)	40 (100)	
cT1aN1M0, stage IIA	6 (8)	0 (0)	
cT1aN2M0, stage IIIA	6 (8)	0 (0)	

CT computed tomography, HRCT high-resolution computed tomography, FDG-PET 18F-fluorodeoxyglucose-positron emission tomography, SUVmax the maximal standardized uptake value

as cIIIB or cIV with distant metastases, which is a contraindication for curative surgery.

FDG-PET also detected previously unrecognized synchronous double malignancies in three of 78 patients (3.8%), including head and neck cancer in two patients and renal cell carcinoma in one patient. Curative treatment was performed in all of these patients.

#### Surgical procedures and pathological diagnoses

Table 3 shows surgical procedures and histopathological diagnoses. Macroscopic complete resection was performed in all 118 patients. No significant differences in the surgical procedures, nodal dissection, or histological type were found between the two groups. Fourteen patients received adjuvant chemotherapy (pIA NSCLC in six patients as a clinical trial, pIIIA NSCLC in four patients, and SCLC in three patients). The pathological stage in the CT/PET group was pIA disease in 66 patients, pIB in eight patients, pIIA in one patient, and pIIIA in three patients. In the CT group, the pathological stage was pIA disease in 28 patients, pIB in eight patients, and pIIIA in four patients.

**Table 3** Surgical procedure and pathological diagnosis

	CT/PET group N = 78	CT group N = 40	P value
Surgical procedure (%)			0.886
Lobectomy	42 (54)	24 (60)	
Segmentectomy	16 (21)	7 (17.5)	
Wedge resection	20 (26)	9 (22.5)	
Lymph node dissection (%)			0.249
SND	37 (47)	25 (62.5)	
MLN sampling	21 (27)	6 (15)	
None	20 (26)	9 (22.5)	
Adjuvant chemotherapy (%)			0.770
Yes	10 (13)	4 (10)	
No	68 (87)	36 (90)	
Pathological findings			
Histology (%)			0.272
Adenocarcinoma	51 (65)	29 (72.5)	
Squamous cell carcinoma	21 (27)	6 (15)	
Large cell carcinoma	2 (2.6)	2 (5)	
Adenosquamous carcinoma	1 (1.3)	0 (0)	
Pleomorphic carcinoma	1 (1.3)	0 (0)	
Carcinoid	1 (1.3)	0 (0)	
Small cell carcinoma	1 (1.3)	3 (7.5)	
pT factor (%)			0.076
pT1a	67 (86)	30 (75)	
pT2a <sup>a</sup>	11 (14)	8 (20)	
pT3 <sup>b</sup>	0 (0)	2 (5)	
pN factor (%)			0.474
pN0	74 (95)	36 (90)	
pN1	1 (1.3)	1 (2.5)	
pN2	3 (3.8)	3 (7.5)	
Pathological stage (%)			0.161
IA	66 (85)	28 (70)	
IB	8 (10)	8 (20)	
IIA	1 (1.3)	0 (0)	
IIIA	3 (3.8)	4 (10)	

SND systematic lymph node dissection, MLN mediastinal lymph node, LN lymph node

<sup>a</sup> Tumor 2 cm or less in greatest dimension with visceral pleural invasion

<sup>b</sup> Primary tumor 2 cm or less in greatest dimension with separate tumor nodule in the same lobe as the primary

Among the 12 patients diagnosed with cN1 or cN2 disease according to FDG-PET results, only four patients (33.3%) were pathologically diagnosed as having pN1 or pN2 disease (Fig. 1); the other eight patients were pathologically diagnosed as having pN0 (i.e., overestimated on FDG-PET) (Fig. 2). The diagnostic accuracy of the preoperative radiographic staging was 78.2% for the CT/PET group and

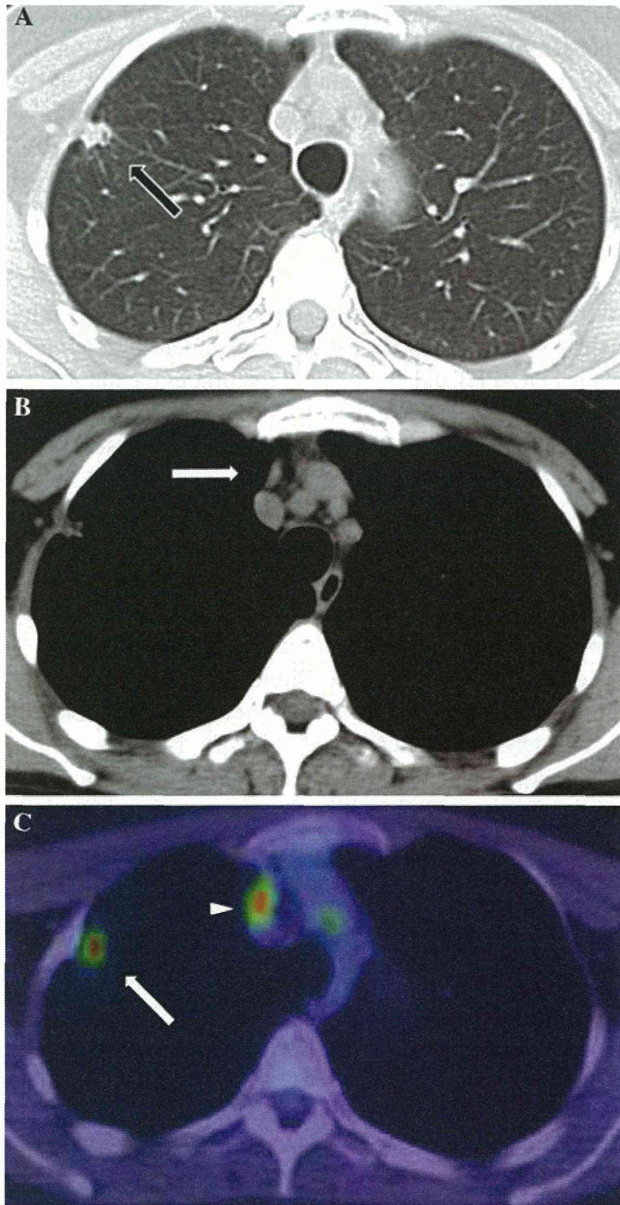


**Fig. 1** A 50-year-old woman with large cell carcinoma, pT1aN2M0, stage IIIA Axial CT image shows 1.2-cm solid nodule (*arrow*) in right upper lobe (**a**). Prevascular lymph node (#3a) is not enlarged (**b**). FDG-PET image shows hypermetabolism at right upper lobe nodule (*arrow*) (SUVmax = 15.7) and #3a lymph node (*arrowhead*) (SUVmax = 5.4) (**c**). Right upper lobe nodule was confirmed to be large cell carcinoma and mediastinal lymph node to be metastasis

70.0 % for the CT group. No significant difference was observed between the two groups (Table 4).

**Outcomes**

The median postoperative follow-up period was 50.3 months (range, 0.7–105.7 months) in the CT group as opposed to 33.0 months (range, 4.9–63.8 months) in the CT/PET group ( $P < 0.001$ ). For the 40 diagnosed with cIA disease

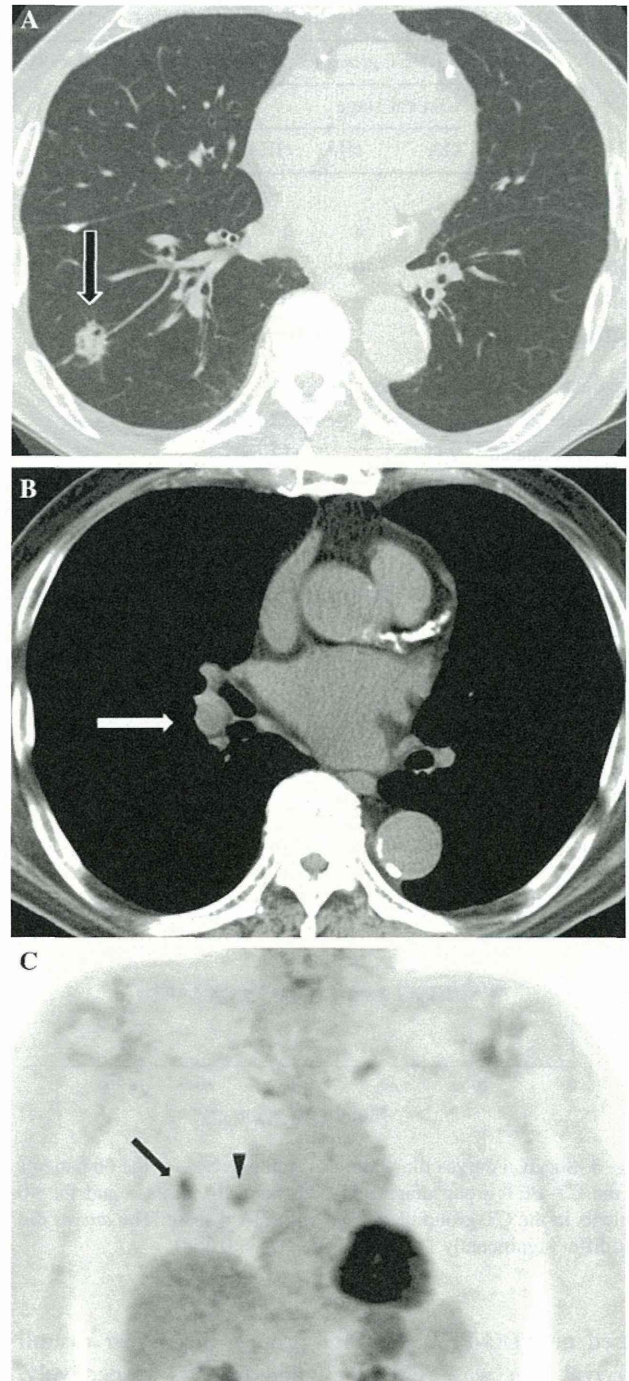


**Fig. 2** An 80-year-old man with adenocarcinoma, pT1aN0M0, stage IA Axial CT image shows 1.8-cm solid nodule (*arrow*) in right lower lobe (**a**). Interlobar lymph node (#11i; *arrow*) are slightly enlarged (short axis; 8 mm) (**b**). FDG-PET image shows hypermetabolism at right lower lobe nodule (*small arrow*) (SUVmax = 3.7) and #11i lymph node (*arrowhead*) (SUVmax = 3.1) (**c**). Right lower lobe nodule was confirmed to be adenocarcinoma, and interlobar lymph node turned out to be chronic granulomatous inflammation

based on CT only (CT group), the 66 patients diagnosed with cIA disease based on both CT and FDG-PET (CT/PET group), and the 12 diagnosed with cIIA or cIIIA disease